STATE RESEARCH CENTER OF RUSSIA

INSTITUTE FOR HIGH ENERGY PHYSICS

IHEP 98-54

A.A. Bogdanov[1], V.A. Korotkov[2], S.B. Nurushev[2], V.A. Okorokov[1],
K.E. Shestermanov[2], M.N. Strikhanov[1], A.N. Vasiliev[2]

THE INCLUSIVE NEUTRAL PION POLARIMETER FOR HIGH ENERGY ACCELERATORS/COLLIDERS

[1] Moscow Engineering Physics Institute, 115409, Moscow, Russia
[2] Institute for High Energy Physics, 142284 Protvino, Russia

Protvino 1998

UDK 539.1.07 M–24

Abstract

Bogdanov A.A., Korotkov V.A., Nurushev S.B. et al. The Inclusive Neutral Pion Polarimeter for High Energy Accelerators/Colliders: IHEP Preprint 98-54. – Protvino, 1998. – p. 16, figs. 9, tables 2, refs.: 15.

The inclusive π^o polarimeter (INPP)is proposed for the oncoming polarized RHIC collider and for the proton ring of accelerator HERA (if polarized). The attractive features of such a polarimeter are a high counting rate, a high analyzing power, a complete azimuthal coverage. It fits also the requirements to be applicable over a large energy region starting at the injection energy and lasting up to the top accelerator/collider energy, as well as to be readjustable for fixed target and collider modes of operations. A sketch of simple apparatus for the INPP application is proposed and the running time estimates are given for polarized RHIC and polarized HERA-p assuming that the analyzing power is the same as it was measured by Fermilab E704 Collaboration and it does not vary with initial energy.

Аннотация

Богданов А.А., Коротков В.А., Нурушев С.Б. и др. Инклюзивный нейтральный пионный поляриметр для ускорителей/коллайдеров высоких энергий: Препринт ИФВЭ 98-54. – Протвино, 1998. – 16 с., 9 рис., 2 табл., библиогр.: 15.

Для вступающего в строй поляризованного коллайдера RHIC и протонного кольца ускорителя HERA-p (поляризованного) предлагается инклюзивный π^0 поляриметр (INPP). Привлекательными особенностями такого поляриметра являются: большая скорость счета, высокая анализирующая способность, полный охват по азимутальному углу. Такой поляриметр отвечает также таким требованиям как применимость в широком интервале энергий, начиная от энергии инжекции до конечной энергии ускорителя/коллайдера, возможность перестройки от моды фиксированной мишени к коллайдерной моде и наоборот. Предлагается схема простой аппаратуры для INPP и выполнены оценки времени измерений поляризаций пучков на RHIC и HERA-p в предположении, что анализирующая способность не зависит от начальной энергии и совпадает с измеренной в эксперименте E704.

1. Introduction

Spin physics investigation with initially polarized colliding nucleons is a very valuable tool for studying the nucleon spin structure and underlying interaction dynamics. Such programme was approved at RHIC [1], [2] and it is under discussions at HERA-p [3], [4]. The future of the hadron spin physics essentially depends on the acceleration of the polarized proton/antiproton beam by making use of the Siberian Snake technique [5]. For measuring the beam polarization during a passage through strong depolarizing resonances (at the acceleration stage) and at the top energy (physics run) one needs to apply a polarimeter with a high factor of merit, M, [6]. According to the classification of polarimeters introduced in [7] the best choice would be the absolute, local and on-line polarimeter. But such a polarimeter sensitive to an accelerator environment has not been established yet. In each practical case, like the polarized RHIC and HERA-p, we are looking not only at M, but also at a cost of such a device. Stemming from this approach the inclusive charged pion polarimeter has been recently proposed in paper [8]. This proposal bases on the high analyzing power, $A_N^{(\pm)}$, discovered by E-704 Collaboration at Fermilab [9]. In the current paper we propose, basing on the A_N^0 measurement by the same Collaboration [10], to apply the inclusive neutral pion polarimeter (INPP) to the RHIC and HERA-p environments. We argue that a high analyzing power and a large cross-section are very attractive features of such a polarimeter. Some additional advantages like full azimuthal coverage, easy fit to the accelerator/collider environments, the background suppression by selecting the high energy threshold for the photon detection, the possible way of building an on-line operation scheme are being discussed too. The estimate of radiation level expected in the INPP at RHIC is also presented.

2. The inclusive π^0 analyzing power

The result of the E704 measurement of analyzing power for the inclusive π^o production in pp-collisions at 200 GeV/c is shown in Fig.1. As it is seen from Fig.1a, $A_N(x_F)$ is practically zero in the range $0 < x_F \leq 0.3$ and an onset of nonzero values appears at $x_F = 0.4$. Then $A_N(x_F)$ rises linearly with x_F in the interval from $x_F = 0.4$ to 0.8 and reaches $A_N(x_F) = 0.15 \pm 0.03$ at $x_F = 0.8$. If we use for polarimetry (for determination of the beam polarization) the last 3 points, then we can write

$$\bar{P}_B = \sum_{i=1}^{3} w_i P_{Bi} / \sum_{i=1}^{3} w_i, \tag{1}$$

where P_{Bi} is a value of the beam polarization extracted from the measurements at the point i; w_i is a weight of point i (in our case $w_i = (1/\Delta P_{Bi})^2$). The relative error, $\Delta P_B/P_B$, in the polarization measurement (assuming that the beam polarization does not depend on i and the raw asymmetry precision, $\Delta\epsilon$ ($\epsilon = A_N \cdot P_B$), is negligible in comparison with ΔA_N) can be found through the relation

$$\Delta P_B/P_B = 1/\sqrt{\sum_{i=1}^{3}(A_{Ni}/\Delta A_{Ni})^2}. \tag{2}$$

Taking the face values of the analyzing power $A_N(x_F)$ from [10], one can conclude that the E704 data allow one to define the beam polarization with the precision

$$\Delta P_B/P_B = \pm 9\%. \tag{3}$$

The systematic error introduces a contribution of the same order of magnitude as it is seen from Fig.1b.

In order to select the applicable p_T region for $A_N(p_T)$, one can use the E704 data presented in Fig.1c. The full circles correspond to the region $0 < x_F < 0.3$, while open squares – o $0.5 < x_F < 0.8$. To keep the analyzing power $A_N(p_T) \geq 5\%$, one needs to limit the useful p_T region by $p_T \geq 0.6$ GeV/c. Therefore, for the application of INPP the following useful region is selected

$$\begin{aligned} &0.4 < x_F < 0.8, \\ &0.6 < p_T(GeV/c) < 2.0, \end{aligned} \tag{4}$$

assuming that all the π^0 mesons produced out of this region present a background.

There are no additional experimental data on analyzing power A_N for inclusive π^0 in pp-collisions in the kinematical region of interest. Therefore, we assume that A_N does not depend on an initial energy and it is the same as in Fig.1a for the same kinematical domain.

3. The scheme of the inclusive neutral pion polarimeter

The scheme of the proposed detectors is shown in Fig.2. The detectors are supposed to be installed in 2 o'clock straight section of RHIC (Fig.2a) or in a suitable place in HERA-p (Fig.2b). It is preferable to install the INPP at the RHIC Interaction Point (IP). In this case in the Fixed Target (FT) mode one can calibrate either *beam1* or *beam2* by using two symmetrically placed INPPs around the IP. As an internal target we plan to use the hydrogen gas target with density $3 \cdot 10^{13}$ $atoms/\mathrm{cm}^2$ [11]. During the main RHIC run (colliding beam (CB) mode) one can continuously monitor beam polarizations by both INPPs. There is a limitation ± 7 m in a free space around IP which may influence on the detector's position.

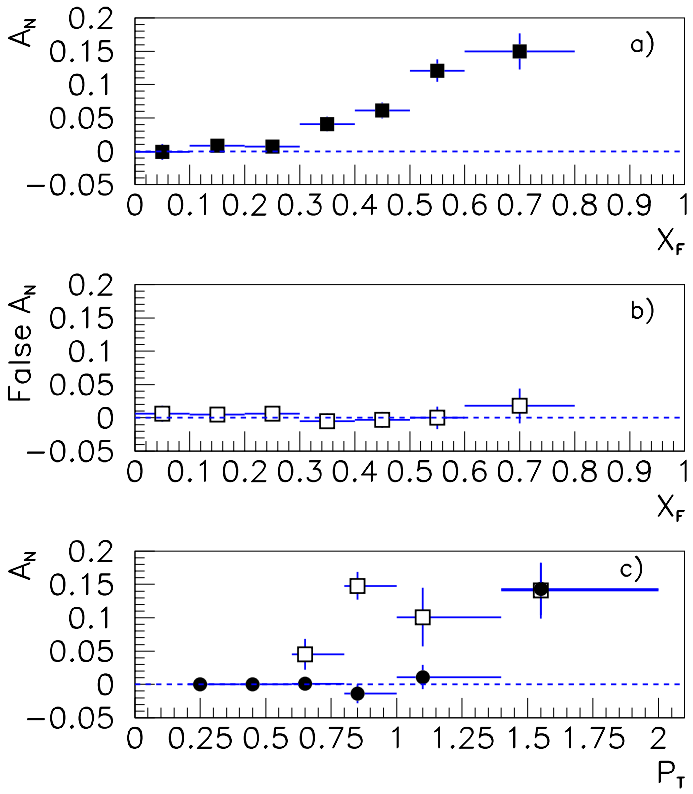

Fig. 1. The analyzing power, $A_N^o(x_F)$, of inclusively produced neutral pions, measured at 200 GeV/c by E704 Collaboration at Fermilab: a) versus x_F, b) a fake asymmetry versus x_F, c) asymmetry versus p_T for two groups of events: closed circles – for $0 < x_F < 0.3$ and open squares – for $0.5 < x_F < 0.8$.

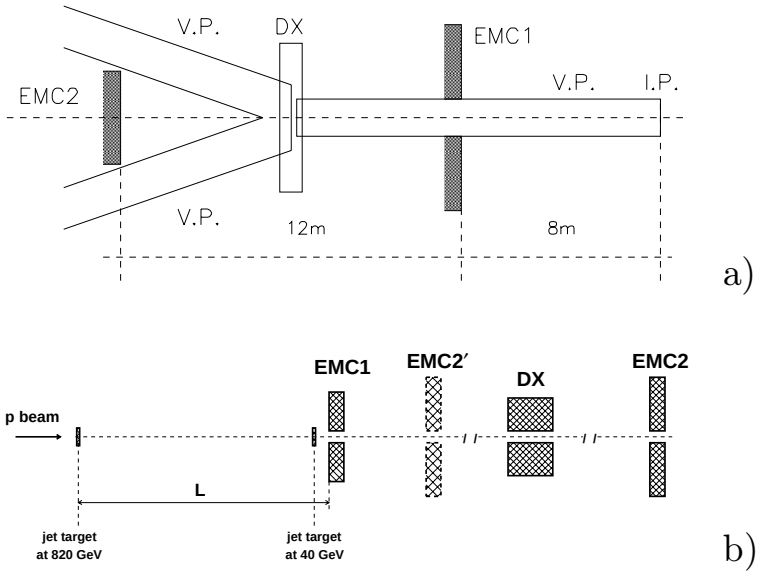

Fig. 2. Layout of the inclusive neutral pion polarimeter at 2 o'clock interaction section of RHIC(a) and for HERA-p(b). EMC1 and EMC2 are the electromagnetic calorimeters. DX is the beam crossing dipole magnet.

The INPP consists of two Electro-Magnetic Calorimeters EMC1 and EMC2. The EMC1 has a hole of diameter $D_1 = 60$ mm defined by a vacuum pipe (V.P.). The EMC2 is placed either in the front or in the rear part of the DX magnet and aims to cover a hole in the EMC1 completely. The DX magnet presents one of the bending magnets belonging to accelerator/collider and placed just at the end of straight section. Depending of its position the EMC2 may have the same hole as EMC1 has or may not have such a hole at all. In such a way the EMC1 and the EMC2 together present one integrated EMC covering the whole azimuthal angle and subtending with high efficiency the useful kinematical interval (4). Such EMC resembles somehow the E704 calorimeter (CEMC) configuration [10] but exceeding the last one twice in an azimuthal acceptance. Moreover, the central part of CEMC, that is the EMC2, can be removed from the beam and put behind the DX magnet. Therefore, it is not radiated by the direct beam and one may hope that the charged secondary particles will not reach it due to a strong magnetic field of DX. The combination of two calorimeters offers some flexibility for an on-line scheme of the INPP as we'll see later.

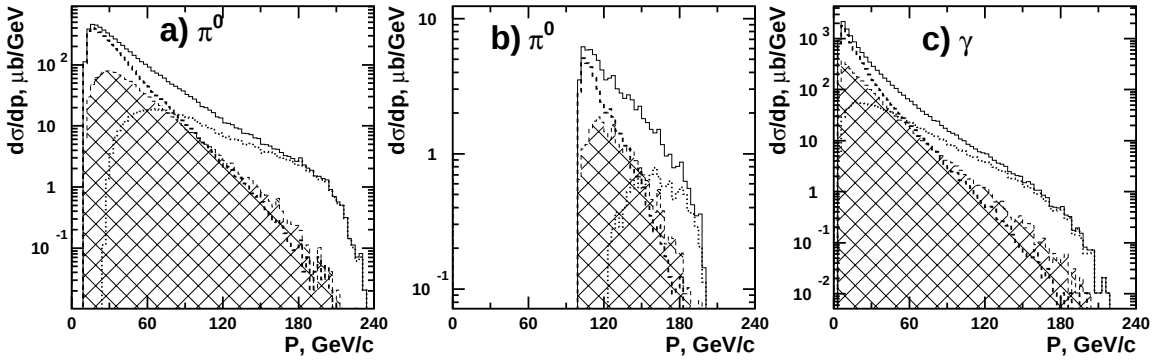

Fig. 3. Cross section of inclusive π^o production in pp interaction at 250 GeV in Fixed Target mode (Fritiof 7.02). Both decay photons are registered in some combination of EMC1 and EMC2. a) versus momentum of produced π^o; b) the same as a) but all π^o's produced in the kinematical region $0.4 < x_F < 0.8$, $0.6 < p_T < 2.0$ GeV/c; c) decay photon momentum spectrum corresponding to π^o's shown in a).

For the separation of photon shower from charged particle shower, each EMC1 and EMC2 are supplied with scintillating hodoscopes installed in front of them (they are not shown in Fig.2). These hodoscopes will also carry another important feature: they measure a time of flight of charged particles accompanying the neutral pion and such information can be useful for suppression of background events.

The inclusive π^o production in the reaction

$$p + p \to \pi^o + X, \tag{5}$$

for the energy region of interest was studied using Monte-Carlo program FRITIOF-7.02 [12]. The cross-sections for reaction (5) at 250 GeV in Fixed Target mode versus different variables are presented in Fig.3. Four kinds of distributions are shown in this figure:

- solid line – both photons are in the acceptance of EMC=EMC1+EMC2;
- dashed line – both photons are in the acceptance of EMC1;
- dotted line – both photons are in the acceptance of EMC2;
- hatched area – one of the photons is in the acceptance of EMC1, while the second one is in the acceptance of EMC2.

All distributions fall steeply in region of interest. Fig.3b is obtained after matching conditions (4). Only small portion of all π^0 mesons is useful for polarimetry. The hatched area presents the case when one gamma from π^o-decay goes to one detector, let say to EMC1, while the second gamma strikes another detector, that is EMC2. Such combination is very important, since it may result in building an on-line INPP. The reason is that we can make a coincidence of signal S1 from EMC1 and S2 from EMC2. We can play on the following features of such combination:

- signal S2 coming from EMC2 should correspond to very energetic π^o (photons). Therefore we can make a fast analog sum of all counters in EMC2, put sufficiently high threshold on energy E_2^{th} ($x_F \sim 0.4$) and use this signal as a trigger. The fact that EMC2 is far from IP and stays behind strong magnetic field of DX (in the main CB mode) assures that signal S2 will be prevailed by photons from π^o decay, that is, S2 must be a clean trigger;
- signal S1 corresponds to the softer photons and by selecting the appropriate energy threshold out one can suppress significantly the backgrounds;
- we can play on E_1^{th} and E_2^{th} in order to optimize a π^o trigger;
- we can build a fast high p_T trigger similar to that used by E704 [10]. A cut on $p_T = 0.6$ GeV/c might be very useful to suppress fake events;
- a special fast processor may be developed at the later stage in order to apply a cut in the π^o mass region by using a relation

$$m_{\pi^o}^2 \simeq E_1 \cdot E_2 \cdot \Theta_{12}^2, \tag{6}$$

where E_1 and E_2 are shower energies deposited in EMC1 and EMC2 correspondingly, Θ_{12} is an opening angle between two photons. All these values are accessible for on-line analysis. Fig.3c shows the distributions of γ's from all produced π^o mesons. In the following we study a possible way of INPP optimization with the goal to apply it to the polarized RHIC and HERA-p.

3.1. The INPP optimization for RHIC

The experimentally measured asymmetry, ϵ, depends on the beam polarization, P_B, the analyzing power of the reaction, A_N, and the purity of selected π^o sample, $d = S/(S+B)$, where S means the number of π^o mesons produced in region (4) and B presents the backgound contribution, in the following way:

$$\epsilon = A_N \cdot P_B \cdot d. \tag{7}$$

From this relation one can extract the magnitude of P_B and estimate its dispersion

$$\sigma^2(P_B) = \frac{1}{(A_N \cdot d)^2 \cdot \sigma_s \cdot \mathcal{L}}. \tag{8}$$

Here, σ_s is the inclusive π^o cross section integrated over region (4), $\mathcal{L} = L \cdot T$ is an integrated luminosity, L is a machine luminosity and T is a running time. As it is seen from the above relation, to reach a minimum dispersion one must get a maximum value of the factor of merit

$$M = (A_N \cdot d)^2 \cdot \sigma_s. \tag{9}$$

If one requires that the beam polarization with a precision ΔP_B be measured, it is necessary to accumulate the statistics

$$N_t = \frac{1}{(A_N \cdot \Delta P_B \cdot d)^2}. \tag{10}$$

The time, t, for gathering N_t events is

$$t = N_t/n, \tag{11}$$

where $n = L \cdot \sigma_s$ is a counting rate.

In further discussion we limit ourselves to the case when each of the two photons is detected by the different calorimeters. The optimization of the INPP parameters was made by looking for the maximum of the factor of merit, M, as a function of two variables: a) distance L from IP to EMC1 and b) photon detection threshold E_γ^{min}. In the latter case both detector thresholds were put the same for simplicity. The diameter of the EMC1 hole was taken as $D_1 = 6$ cm. Fig.4 presents the results of such calculations for the FT mode at 250 GeV RHIC energy, while for CB mode they are presented in Fig.5. One can see that in both cases there is a clear maximum in M versus L and the shape of the curves resembles a gaussian. The curve falls down on the left side of the maximum due to a decreasing analyzing power, while on the right side of the maximum it drastically drops because of a sharp decrease of the useful cross section, σ_s. The magnitude of M strongly depends on the threshold photon energy changing by one order of magnitude when passing from $E_\gamma^{min} = 25$ GeV to 55 GeV. The position of maximum weakly depends on this cut (changing from L=5m to 5.6 m). The maximum threshold energy was taken in accordance with condition (4) in order to avoid a cut of the useful events. For a cut at $E_\gamma^{min} = 55$ GeV the optimum position of EMC1 in the FT mode is L = 5.6 m and $M \simeq 1.7 \cdot 10^{-1}$ μb (see Fig.4a). Comparison with Fig.5a for the CB mode shows that this position does not practically depend on the mode of RHIC running.

In passing from the top energy to the injection energy, $E_{inj} = 23$ GeV, one sees a change in the optimum position of EMC1 (see Fig.6a). The change is roughly proportional to the energy variation and this fact is understandable through the kinematics of the production and decay of π^0 mesons. The shape of the figure is not changing almost. In the CB mode (Fig.7) for the injection energy all distributions are the same as above for the FT mode. For the highest threshold $E_\gamma^{min} = 5$ GeV corresponding to condition (4), the

optimum position of EMC1 is L=0.52 m and $M \simeq 2 \cdot 10^{-1}$ μb which is higher by one order of magnitude than at the lowest threshold $E_\gamma^{min} = 2$ GeV (Fig.6a and 7a). Therefore, we can conclude that the INPP can be effectively used in the FT and the CB modes of RHIC, as well as at top and injection energies. In the latter case one must deplace EMC1 from L=5.6 m to 0.52 m. Figs.4-7 present also the dependences of some other useful observables versus the distance L. For example, for the FT mode at 250 GeV, Fig.4b shows the ratio of signal S to signal plus background (S+B). At L=5.6 m and $E_\gamma^{min} = 55$ GeV the ratio $S/(S+B) \simeq 0.9$ meaning that one expects 90% of useful events and $\simeq 10\%$ of backgrounds. The useful cross section for accepted cuts can be found from Fig.4c and it is equal to $\sigma_s = 12\mu b$. The expected analyzing power comes from Fig.4d and equals $A_N \simeq 10\%$. If we want to attain 5% precision in the beam polarization measurement, we can calculate now all the parameters by using the above given relations and assuming the luminosity $\mathcal{L}$=13 $(\mu b)^{-1}$ for the FT mode. The results of the calculations are presented in Table 1. It is seen that the required precision in the beam polarization can be reached in ~ 10 minutes. The last two rows of Table 1 present the expected outer diameters of calorimeters which permit to accept 99% of photons from π^0 decay. Similar calculations were done for the colliding mode at $\sqrt{s} = 500 GeV$. Fig.5 presents the results of such calculations and shows the similar to Fig.4 behaviour for any of the observables. From these data one can fill in Table 1 for this energy. As it is seen from Table 1, the INPP parameters in the CB mode are close to those in the FT mode, but the time of the polarization measurement is much shorter due to the higher luminosity of the colliding beams. The gross sizes of the calorimeters are virtually the same as in the FT mode.

Table 1. **The Inclusive Neutral Pion Polarimeters Parameters**

Parameters	**RHIC**				**HERA-p**	
E, GeV	250	250 + 250	23	23 + 23	40	820
L, m	5.6	5.5	0.5	0.5	1.0	17.5
S/S+B	0.90	0.90	0.90	0.90	0.68	0.84
σ_s, μ b	12	10	15	13	13	10
n, counts/sec	156	2000	195	260	195	150
A_N, %	10	10	10	10	8.0	9.0
$N_{5\%}(10^4)$	9	10	10	10	12	10.1
$T_{5\%}$, min	10	1	9	7	10.3	12
D_{out} EMC1,mm	360	360	300	300	200	200
D_{out} EMC2,mm	300	300	800	800	400	400

The important problem is the measurement of the beam polarization at the injection energy of 23 GeV and the colliding mode at the same initial lab. energy ($\sqrt{s} = 46$ GeV). The results of estimates are presented in Figs.6 and 7. Using these data one can fill in the 4th and 5th columns of Table 1. The main parameters of the INPP are virtually the same as above but two changes are obvious: one must put the EMC1 very close to the IP and make bigger the gross size of the EMC2. For the colliding mode the situation is similar. It is obvious that the INPP can measure the beam polarization at RHIC in the whole range of the beam energy and in both modes of operation.

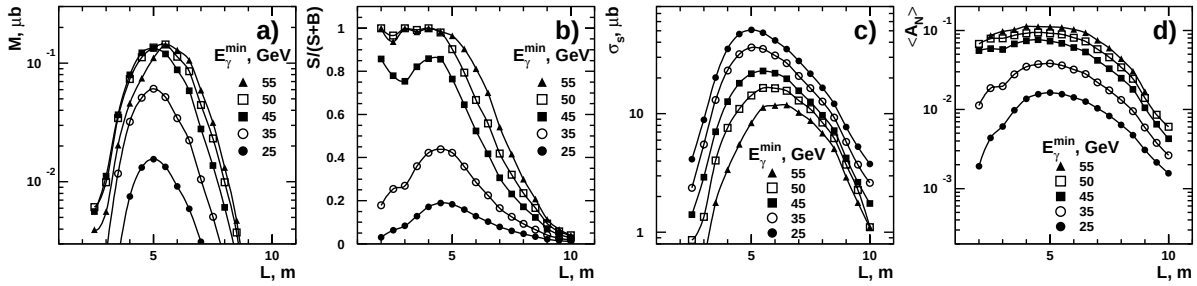

Fig. 4. Shown as a function of EMC1 position, L, are (FT): a) figure of merit, b) the signal significance, c) the integrated useful cross section for inclusive π^0 production, d) the average analyzing power. The initial protons energy is 250 GeV. The curves are labeled by threshold energy, E_γ^{min}, for detection of decay photons in EMC1 and EMC2.

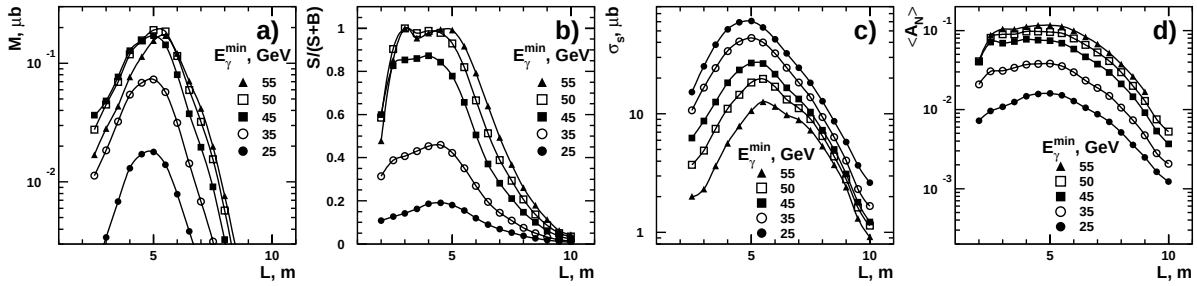

Fig. 5. Shown as a function of EMC1 position, L, are (CB): a) figure of merit, b) the signal significance, c) the integrated useful cross section for inclusive π^0 production, d) the average analyzing power. The initial protons energy (in colliding mode) is 250 + 250 GeV. The curves are labeled by threshold energy, E_γ^{min}, for detection of decay photons in EMC1 and EMC2.

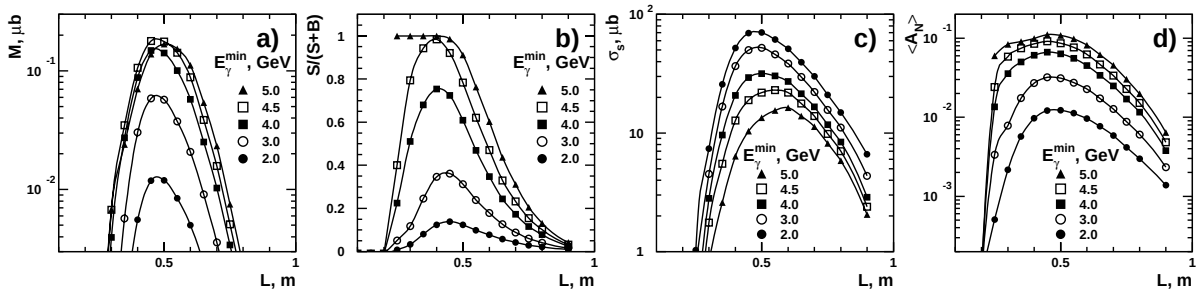

Fig. 6. Shown as a function of EMC1 position, L, are (FT): a) figure of merit, b) the signal significance, c) the integrated useful cross section for inclusive π^0 production, d) the average analyzing power. The initial protons energy is 23 GeV. The curves are labeled by threshold energy, E_γ^{min}, for detection of decay photons in EMC1 and EMC2.

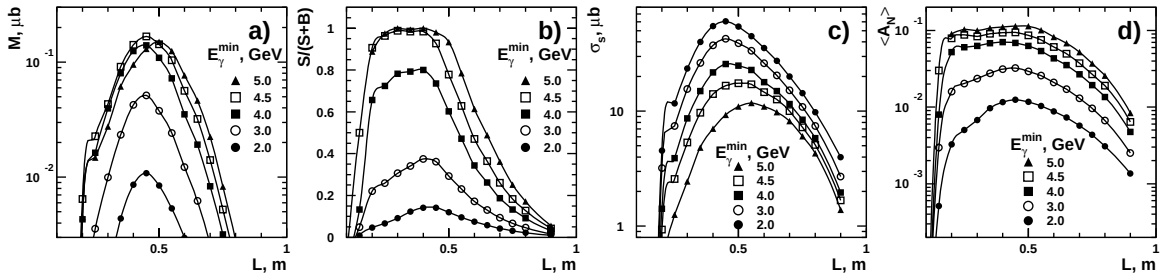

Fig. 7. Shown as a function of EMC1 position, L, are (LB): a) figure of merit, b) the signal significance, c) the integrated useful cross section for inclusive π^0 production, d) the average analyzing power. The initial protons energy (in colliding mode) is 23 + 23 GeV. The curves are labeled by threshold energy, E_γ^{min}, for detection of decay photons in EMC1 and EMC2.

3.2. The INPP optimization for HERA-p

The HERA-p environments have several specific features. It contains only one proton ring, therefore a polarimeter would be used only in a fixed target mode. Second, an energy range includes 40-820 GeV, that is, it spans $20 \times E_{min}$ range, while at RHIC it was $10 \times E_{min}$. Third, the electron and the proton beams are separated at a large distance from IP (around 100 m, while at RHIC two proton beams are separated around 20 m). Therefore, the INPP might be different in size, shape, positions, etc. A sketch of the proposed INPP is shown in Fig.2b; note that this scheme is not connected yet to the HERA lattice structure. The INPP for a top energy of 820 GeV would consist of two electromagnetic calorimeters EMC1 and EMC2 separated by a series of the accelerator magnetic elements (DX in Fig.2b). For separation of the photons from charged particles both EMC1 and EMC2 could be supplied with scintillating hodoscopes (not shown in Fig.2b). The results of calculations of INPP parameters for the HERA-p ring are shown in Fig.8 for 820 GeV. There is a wide maximum in the dependence of figure of merit, M, on L around L=15÷19 m (Fig.8a). The highest magnitude of M is $1.7 \cdot 10^{-1}$ μb and it is reached at L=17 m for E_γ^{min} = 170 GeV. The next Fig.8b shows a plateau in the signal significance, d, versus L in a region 11-16 m and then d drops precipitiously at L>17 m. Combining these data with the useful cross section σ_s presented in Fig.8c one gets an optimum value L=17 m, at which $\sigma_s = 10\mu$b. The estimated INPP parameters for the HERA-p top energy is included in Table 1. One can conclude that the beam polarization precision of 5% can be obtained by the 12' beam run. The parameters of the INPP for the injection energy of 40 GeV were estimated by applying the similar approach to Fig.9. They are presented also in Table 1. It is seen that a precision of 5% in the beam polarization measurement can be reached at the injection energy for approximately the same time as it was for the top energy. The positions of EMC1 vary from 1m at 40 GeV to 17m at 820 Gev, while EMC2 should be deplaced closer to EMC1 at 40 GeV (EMC2' in Fig.2b). This may present a problem since a polarimeter can interfer with the accelerator lattice. A possible solution might be to deplace the internal target as it is shown in Fig.2b. Another interesting conclusion is: the time spent on the beam polarization measurements is virtually the same at RHIC and HERA-p. The gross dimensions of the calorimeters are smaller at HERA-p than at RHIC due to a higher energy of HERA-p.

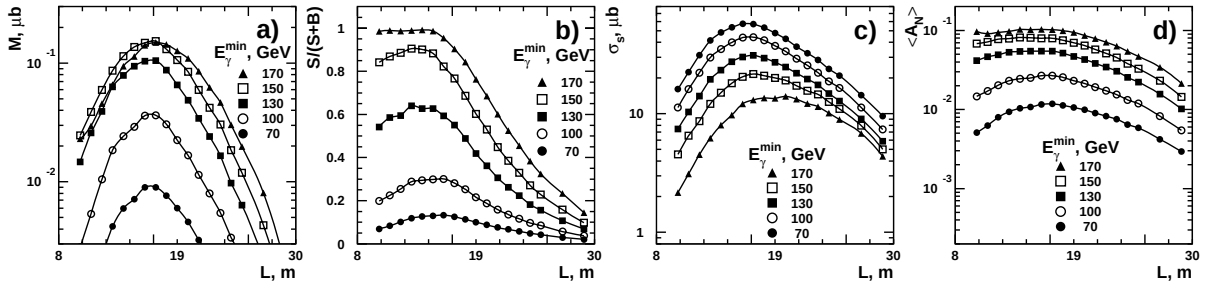

Fig. 8. Shown as a function of EMC1 position, L, are: a) figure of merit, b) the signal significance, c) the integrated useful cross section for inclusive π^0 production, d) the average analyzing power. The initial protons energy is 820 GeV. The curves are labeled by threshold energy, E_γ^{min}, for detection of decay photons in EMC1 and EMC2.

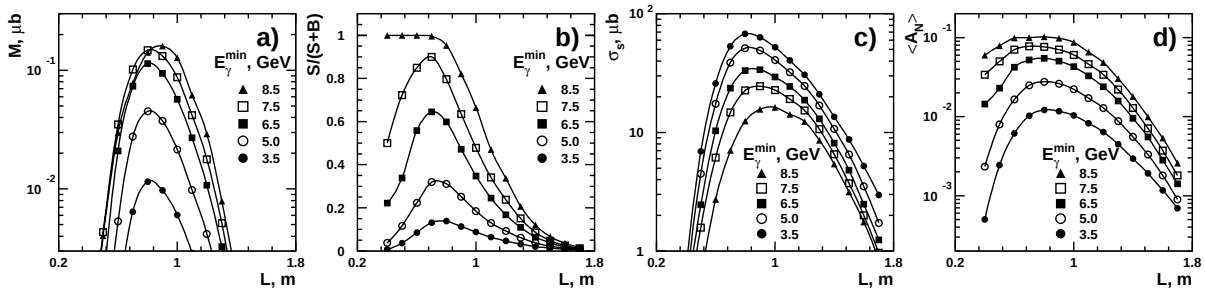

Fig. 9. Shown as a function of EMC1 position, L, are: a) figure of merit, b) the signal significance, c) the integrated useful cross section for inclusive π^0 production, d) the average analyzing power. The initial protons energy is 40 GeV. The curves are labeled by threshold energy, E_γ^{min}, for detection of decay photons in EMC1 and EMC2.

3.3. The kinematical aspects of INPP

The qualitative understanding of the main features of INPP and quick estimates of its parameters can be made by applying the standard π^0 decay kinematics and using the fixed kinematical domain (4). It is important to gently apply those relations to the specific environments. A vacum pipe with diameter D_1 puts a limit for detection angle

$$\tan\Theta_1 = \frac{D_1/2}{L}, \tag{12}$$

where L is a distance from IP to the EMC1. For the fixed π^0 momentum from conditions (4) one can define a minimum production angle, Θ_2, for π^0 at which the useful p_T and x_F domain will be respected

$$\sin\Theta_2 = \frac{\overline{p}_T}{\overline{p}_\pi}, \tag{13}$$

where $\overline{p}_\pi \simeq \overline{E}_\pi$. Assuming $\overline{p}_T = 0.8$ GeV/c, $\overline{x}_F = 0.6$ one gets

$$\sin\Theta_2 = \frac{1.33}{E_p}, \tag{14}$$

where E_p is an initial proton energy. Therefore, for any fixed energy one can find the EMC1 position by putting $\Theta_1 = \Theta_2$ and using the previous relation. For example, if E_p=250 GeV, then $\Theta_2 = 5.3$ mrad. By putting $L = \frac{D_1/2}{\Theta_2}$ for $D_1 = 60$ m, we find $L = 5.6$ m which is close to the number in Table 1 obtained by the precise calculations.

In order to get a rough but quick estimate of the gross size of the EMC1, we must fix a portion, α, of π^0 decay which we'd like to accept. Let us assume $\alpha = 0.99$. From the π^0 decay distribution we get a relation between the α and the largest accepted photon angle around the π^0's direction, Θ_a, that is

$$sin\frac{\Theta_a}{2} = \frac{sin(\Theta_{\gamma\gamma}/2)}{\sqrt{1 - a^2 \cdot \beta^2}}, \tag{15}$$

where β is a π^0 velocity in units of the light velocity and a minimum decay angle, $\Theta_{\gamma\gamma}$, between two decay photons, is defined by relation

$$sin(\Theta_{\gamma\gamma}/2) = \frac{m_\pi}{E_\pi}. \tag{16}$$

Since the electromagnetic calorimeter should be installed symmetrically around the beam axis, we must calculate the largest angle of π^0 emission with large p_T (1.6 GeV/c). Since the largest accepted π^0 angle $\Theta_{\pi^0}^{max}$ comes from the slowest π^0 decay, we put $E_\pi = 0.4 \cdot E_0$. Therefore, the largest angle of the photon emission Θ_{max} is defined by

$$\Theta_{max} = \Theta_a/2 + \Theta_{\pi^0}^{max}. \tag{17}$$

As an example for $E_0 = 250$ GeV, we get $\Theta_{max} = 22$ mrad. At L=5.6 m this leads to the outer diameter of EMC1: $D_{out} = 2 \times 22 \times 5.6 = 246$ mm. By adding the extra size for the shower width of $\simeq 100$ mm one gets $D_{out} \simeq 346$ mm. The more precise calculation gives $D_{out} = 360$ mm (see Table 1). We conclude that the rough but quick estimates of the position and gross size of the electromagnetic calorimeter for INPP can be made by applying the above kinematical relations.

3.4. The radiation level in the INPP at RHIC

The INPP will be exposed to radiation from pp-collisions during the collider operation or from any internal target used for a polarimetry in the FT mode. We assume that the main source of radiation is the two colliding beams (at 250 GeV due to the high luminosity) and neglect any other effects. A radiation dose in the INPP can be estimated following the scheme developed at SSC and described by Particle Data Group (see [13], p. 152). According to this scheme the dose rate at RHIC, $\dot{D}$(RHIC), can be calculated from the dose rate at SSC, $\dot{D}$(SSC), through relation

$$\dot{D}\ (RHIC) = \kappa \cdot \dot{D}\ (SSC), \tag{18}$$

where

$$\kappa = \frac{(L_{nom} \cdot \sigma_{inel} \cdot H \cdot < p_T >^{0.7})_{RHIC}}{(L_{nom} \cdot \sigma_{inel} \cdot H \cdot < p_T >^{0.7})_{SSC}}. \tag{19}$$

Here L_{nom} is a nominal collider luminosity, σ_{inel} is an inelastic total cross section, H is the height of the pseudorapidity plateau, $< p_T >$ is a mean value of transverse momentum of particles of interest (charged hadrons, neutrons and photons). So, $\kappa = 3.1 \cdot 10^{-2}$. The dose rate for SSC is given by the expression

$$\dot{D}\ (SSC) = \frac{0.4 MGy \cdot yr^{-1}}{(r_{\perp}/1cm)^2} = \frac{40 MRad \cdot yr^{-1}}{(r \cdot \sin\theta/1cm)^2}, \tag{20}$$

$r_{\perp}$ is a distance from beam axis to a detector, θ is a polar angle of inclusively produced charged particle. Using as inputs the data from Table 2, one can find the absolute dose rate at RHIC (the relative dose rate for the central plateau is shown in Table 2 in the last row):

$$\dot{D}= \frac{1.3 Mrad \cdot yr^{-1}}{(r \cdot \sin\theta/1cm)^2}. \tag{21}$$

This relation can be applied to the thin detectors, like scintillating hodoscopes irradiated by the charged particles. In a medium like calorimeter one must take into account the hadronic and electromagnetic showers. The most commonly modelled in details calorimeter was a fine-sampling uranium/scintillator calorimeter with alternating 3 mm uranium plates and 3 mm scintillator sheets [14]. For one year irradiation at a nominal SSC luminosity, one expects the following parametrization of the maximum dose (see Fig.7 in [14]):

$$D(Gy \cdot yr^{-1}) = c_1 \cdot \eta^{c_2}, \tag{22}$$

where η is a pseudorapidity, constants c_1 and c_2 depend on the type of particles and the position of the EMC. For example, for SSC at the position of calorimeter L=2 m (from IP) they equal $c_1 = 4.27$ and $c_2 = 9.8728$ for the electromagnetic dose and $c_1 = 5.28 \cdot 10^{-2}$ and $c_2 = 11.2518$ for the hadronic dose. The ratio of the electromagnetic dose to the hadron dose is roughly of order of a ratio of the nuclear interaction length to the radiation length. In order to transform those doses from SSC to RHIC, we must multiply them by $\kappa = 3.1 \cdot 10^{-2}$ for the central plateau. Assuming that EMC1 is placed at L=5.5 m instead of 2 m, we get the final electromagnetic dose at RHIC

$$D(RHIC, el.mag.) = 1.59 \cdot 10^{-2} \cdot \eta^{9.8728}(Gy \cdot yr^{-1}). \tag{23}$$

In a similar way one gets for hadron contribution to dose

$$D(RHIC, hadr.) = 1.98 \cdot 10^{-4} \cdot \eta^{11.2518}(Gy \cdot yr^{-1}). \tag{24}$$

The closest to the beam position of EMC1 is $\eta_{max} = 5.62$ and we get

$$D(RHIC, el.mag.) = 40\ Mrad \cdot yr^{-1}. \tag{25}$$

Such a dose is expected at the maximum of the electromagnetic shower and in the region of the central plateau. At $\eta = 5.6$ this dose must be decreased by a factor of 5 leading to the final maximum dose at EMC1 of 8 $Mrad \cdot yr^{-1}$. In recent research paper [15] it

was shown that the required parameters could be obtained by using the PS-115 based scintillators produced by the injection molding technique. The expected hadronic dose is of order 1 $Mrad \cdot yr^{-1}$ for the same condition (a ratio D(hadron)/D(el.mag.) $\approx \frac{\lambda_{el.mag.}}{\lambda_{hadr}}$). Therefore, it can be practically neglected under our condition. The same is true for the neutron initiated dose.

Table 2. **A rough comparison of beam-collision induced radiation at the different colliders**

Collider	RHIC	Tevatron	LHC	SSC	100TeV
$\sqrt{s}(TeV)$	0.5	1.8	15.4	40	100
$L_{nom}(cm^{-2} \cdot s^{-1})$	$2 \cdot 10^{32}(a)$	$2 \cdot 10^{30}$	$1.7 \cdot 10^{34}$ (a)	$1 \cdot 10^{33}$	$1 \cdot 10^{34}$
$\sigma_{inel}(mb)$	50	56	84	100	134
H	3.0	3.9	6.2	7.5	10.6
$< p_\perp > (GeV/c)$	0.425	0.46	0.55	0.60	0.70
Relative dose(b)	$3.1 \cdot 10^{-2}$	$5 \cdot 10^{-4}$	11	1	20
Comments: a)High luminosity option. b) Proportional to $L_{nom} \cdot \sigma_{inel} \cdot H \cdot < p_\perp >^{0.7}$.					

4. The possible on-line INPP scheme

The following scheme of on-line INPP can be proposed. The EMC counters might be electronically separated in two halves (left-right) for normally polarized proton beam. Pulses from the left counters will be summed independently, as well as from the right counters. This means integration in azimuthal angle in the interval $-90^0 \div +90^0$ for the left half and $90^0 \div -90^0$ for the right one. Let us denote these pulses as L1 and R1. After making a coincidence $S12 = S1 \times S2$, one creates the following coincidences: $S3 = S12 \times L1$ *or* $S4 = S12 \times R1$. S3 and S4 will feed the scalers Sc1 and Sc2. Denoting the counting rates on Sc1 as N1 and on Sc2 as N2, we can define the asymmetries

$$\epsilon_L = \epsilon \cdot \overline{cos\phi} = \frac{N1^+ - N1^-}{N1^+ + N1^-},\ \epsilon_R = \epsilon \cdot \overline{cos\phi} = \frac{N2^+ - N2^-}{N2^+ + N2^-}, \tag{26}$$

where ϵ was defined earlier, $\overline{\cos\phi}$ means an averaged value of $cos\phi$ over the acceptance of the half of EMC1; $N1^{(+,-)}$ presents the counting rates for the up and down beam polarization. The $\overline{\cos\phi}$ equals 0.79 for the indicated above acceptance. Therefore, the amount of needed statistics for reaching 5% in the beam polarization measurement will be higher than before by coefficient $|\overline{cos\phi}|^{-2} = 1.6$. The time of measurement therefore will increase by the same amount. We continue to study this problem in order to realize the on-line regime. There are several problems open at the moment. First one is a shower width that must be taken into account, in particularly, in the on-line regime. This problem can be solved by taking out of a trigger the set of counters surrounding just a vacuum pipe in EMC1 and the outer counters in EMC2. The second problem is relevant to the "diamond" size of the beam in the IP. It may put a severe restriction for a trigger at the lowest energy, when calorimeters are placed close to the IP. This problem must be solved specifically

for each accelerator/collider by Monte-Carlo calculations. The energy calibration of both calorimeters can be done by reconstruction of π^o events and normalizing to the mass of π^o. Additionally EMC1 energy scale may be calibrated by muons or charged hadrons. The LED/Laser and radioactive sources will be used for monitoring calorimeters functioning.

By comparing INPP with ICPP (inclusive charged pion polarimeter), one can outline the following advantages of INPP over ICPP:

- full azimuthal coverage. This allows one to measure any transverse component of beam polarization in the same run;
- practically full coverage of useful x_F range;
- practically full coverage of useful p_T range;
- due to the use of the electromagnetic calorimeter, the INPP becomes more preferable with the growth of energy than the ICPP;
- no necessity for a magnetic spectrometer and extra particle identification. The EMC fulfils all these functions itself.

Conclusions

We propose to use the Inclusive Neutral Pion Polarimeter (INPP) at high energy accelerators/colliders for the following reasons:

- its high analyzing power, A_N;
- its large production cross section, σ_s. Due to these two factors the INPP has a high factor of merit, $\mathrm{M} = (A_N)^2 \cdot \sigma_s$;
- it fits well to the RHIC and HERA-p environments; it can be easily used in the fixed target as well as in the collider modes.
- it serves as a local polarimeter;
- it is a "transparent"(non disturbing) polarimeter allowing one to make a continuous control of beam polarization;
- it may be used as on-line polarimeter;
- it is less sensitive to the background due to the high energy threshold for photons;
- the technique (electromagnetic calorimeters) is robust and reliable.

There are two open problems which must be solved in order to make the INPP a real polarimeter: a) the absence of the precise experimental data on $A_N(\pi^0)$ in the energy range of interest, and b) the necessity to demonstrate in experiment that an INPP can be operated as an on-line polarimeter.

References

[1] Makdisi Y.I. In:*Proc.of 12th Intern. Symp. on High-Energy Spin Physics*, September 10-14, 1996, Amsterdam, The Netherlands, p.107.

[2] Enyo N.,*ibid*, p.118.

[3] M. Anselmino et al., *Workshop on 'Future Physics at HERA'*, Hamburg, 1996, ed. by G. Ingelman, A. de Roeck, R. Klanner, p.837.

[4] V.A. Korotkov, W.-D. Nowak, *Workshop on 'Physics with Polarized Protons at HERA'*, DESY, March-September 1997, ed. by A. De Roeck and T. Gehrmann, p.204.

[5] Derbenev Ya.S. and Kondratenko A.M., DAN 223, 830(1976).

[6] Kuroda K.- In: AIP Conf.Proc., 1983, 95, p.546.

[7] Nurushev S.B. - In: Proc. of Intern.Workshop on Spin Phenomena in High Energy Physics, September 14-17, 1983, Protvino, Russia, p.5.

[8] Mariam F.G. et al.- In: Proc.of 12th Intern. Symp. on High-Energy Spin Physics, September 10-14, 1996, Amsterdam, The Netherlands, p.797.

[9] Adams D.L. et al., Phys.Lett., B264, 462(1991).

[10] Adams D.L. et al., Z.Physik C, 56, 181(1992).

[11] A. Golendoukhin (HERMES Collaboration), The HERMES Polarized Proton Target at HERA. In: Proc. (see [8], p.331).

[12] Hong Pi, *Comp. Phys. Comm. 71, 173(1992).*

[13] Particle Data Group, Phys. Rev. 54D, 152(1996).

[14] Groom D.E.- Radiation Levels in SSC Detectors. In: Proc. of the Summer Study on High Energy Physics in the 1990's, June 27-July 15, 1988 Snowmass, Colorado, ed. Sh. Jensen, p. 711.

[15] Vasil'chenko V.G., Lapshin V.G., Peresypkin A.I., et al., Nucl. Instr. Meth. in Physics Research A 369(1996) 55.

Received August 9, 1998

А.А.Богданов, В.А.Коротков, С.Б.Нурушев и др.
Инклюзивный нейтральный пионный поляриметр для ускорителей/коллайдеров высоких энергий.

Оригинал-макет подготовлен с помощью системы LaTeX.
Редактор Е.Н.Горина. Технический редактор Н.В.Орлова.

Подписано к печати 07.08.98. Формат 60 × 84/8. Офсетная печать.
Печ.л. 1,87. Уч.-изд.л. 1,44. Тираж 180. Заказ 252. Индекс 3649.
ЛР №020498 17.04.97.

ГНЦ РФ Институт физики высоких энергий
142284, Протвино Московской обл.

Индекс 3649

П Р Е П Р И Н Т 98-54, И Ф В Э, 1998